World Journal of Advanced Engineering Technology and Sciences
eISSN: 2582-8266
Cross Ref DOI: 10.30574/wjaets
Journal homepage: https://wjaets.com/

(RESEARCH ARTICLE)

Check for updates

Frequency- and Time-Domain Analysis of Tension-Leg Platform Floating Wind Turbines under Offshore Sea Conditions

Alabo Abiye Ekine *, Blessed Godstime Nwoka and Samson Nitonye

Department of Marine and Offshore Engineering, Faculty of Engineering, Rivers State University, Port Harcourt, Nigeria.

World Journal of Advanced Engineering Technology and Sciences, 2026, 18(02), 216-229

Publication history: Received on 09 January 2026; revised on 16 February 2026; accepted on 19 February 2026

Article DOI: https://doi.org/10.30574/wjaets.2026.18.2.0101

Abstract

Floating offshore wind turbines on tension-leg platforms (TLP-FOWTs) face critical design challenges due to complex coupled dynamic behavior, which, if inaccurately predicted, risks over-design or structural failure. This study aimed to develop and validate an integrated aero-hydro-servo-elastic OpenFAST model for TLP-FOWTs and establish a clear two-stage methodology linking efficient frequency-domain screening with detailed non-linear time-domain verification. The coupled model was developed using potential flow theory, Morison's equation, Blade Element Momentum theory, and linear tendon stiffness, with frequency-domain analysis identifying natural modes and time-domain simulations performed under operational and 50-year extreme storm conditions. Frequency-domain results revealed a resonant platform pitch mode at 0.142 Hz, yielding a peak Pitch RAO of 1.65 deg/m at 0.143 Hz. Time-domain simulations under extreme storm conditions (Hs=14m, Tp=16s) produced a maximum platform pitch of 12.7°, a tower base bending moment of 245 MNm, and a critical minimum tendon tension of 5.1 MN—a 65% reduction from pretension indicating near-slack risk. Model validation against benchmark data showed excellent agreement, with deviations below 7% and only 3.1% difference at the resonant peak. This study concludes that resonant pitch motion is the primary driver of extreme loads and tendon slackness risk in TLP-FOWTs, and that the integrated two-stage framework enhances design reliability and cost-effectiveness. It is recommended that designers prioritize pitch resonance avoidance and tendon slackness checks, and consider increasing tendon pretension or modifying platform geometry for sites where 50-year minimum tensions approach critical limits.

Keywords: Floating Offshore Wind Turbine (FOWT); Coupled dynamic analysis; Frequency-domain analysis; Time-domain simulation; Tendon tension integrity

1. Introduction

The global shift towards sustainable energy has placed offshore wind power at the forefront of renewable energy development. Winds over the ocean are stronger and more consistent than on land, offering the potential for greater power generation (Kusumo, 2021). Initial research and design efforts have effectively established methodologies for fixed-bottom offshore wind turbines, including site-specific analyses for power generation and structural performance (Joseph et al., 2022). To harness this resource in water depths where traditional fixed-bottom structures become impractical, floating offshore wind turbines (FOWTs) are essential. Among the various floating platform designs, the Tension-Leg Platform (TLP) presents a highly stable option. A TLP is secured by vertically taut mooring lines, or tendons, which greatly restrict its heave, pitch, and roll motions. This stability is advantageous for the operation and structural integrity of the wind turbine mounted on it (Mendoza, 2022).

However, the design of a TLP supporting a wind turbine is a complex engineering challenge. The complete system is subjected to a combination of dynamic loads from wind, waves, and currents. These forces are not independent; they interact in a coupled manner. The motion of the platform induced by waves alters the relative wind speed seen by the

* Corresponding author: Ekine Alabo Abiye

rotor, which in turn changes the aerodynamic loads. This feedback loop between the aerodynamic and hydrodynamic systems must be captured for accurate prediction of loads and motions (Santoso, 2023). Therefore, analyzing the turbine and platform as separate, uncoupled systems—an approach more common in preliminary fixed-bottom analyses—can lead to incorrect and potentially unsafe design predictions for floating systems.

Engineers use two primary computational methods to analyze these dynamics: frequency-domain and time-domain analysis. Frequency-domain analysis is a powerful tool for initial design stages. It provides a efficient way to understand how the system responds to different wave frequencies, helping to identify natural frequencies and potential resonance issues early in the design process (Chen & Hu, 2020). Time-domain analysis, on the other hand, involves simulating the actual response of the structure over a period. This method is crucial for capturing non-linear events, such as large amplitude motions, viscous drag effects, and the detailed progression of extreme storm conditions (Pratama, 2021). A comprehensive understanding of TLP floating wind turbine behavior requires the strategic application of both methods. This study will develop an integrated model to perform both types of analysis, contributing to safer and more economically viable designs for deep-water wind energy.

The high cost of floating offshore wind energy remains a major barrier to its widespread adoption. A significant portion of this cost stems from uncertainty and risk in the engineering design phase. Predicting the exact behavior of a floating wind turbine in the harsh offshore environment is difficult. The core problem lies in the complex, coupled interaction between the wind turbine and the floating platform. Using simplified models that do not properly account for this coupling can result in two unfavorable outcomes: an over-designed, excessively heavy, and costly structure, or an under-designed structure prone to premature failure or unsafe operation.

The engineering community lacks a clear, standardized methodology that efficiently links preliminary frequency-domain screening with detailed time-domain verification specifically for TLP-type floaters. Designers may rely too heavily on one method without fully leveraging the strengths of the other, leading to either inefficient designs or missed critical load cases. This knowledge gap creates financial risk for project developers and investors. Uncertainty in load prediction can inflate contingency costs and make it harder to secure financing, ultimately slowing down the deployment of this valuable clean energy technology. This research aims to address this problem by creating and demonstrating an integrated analytical model that bridges these two essential analysis domains for TLP floating wind turbines.

Research into floating offshore wind turbines has evolved rapidly from conceptual feasibility studies to sophisticated dynamic response analysis and pilot-scale demonstrations. Initial investigations heavily borrowed concepts from the offshore oil and gas industry, but the unique challenges posed by a tall, rotating wind turbine on a floating base have spurred dedicated research streams. Numerous studies have systematically examined different floating platform archetypes such as Spar, Semi-submersible, and TLP evaluating their motion characteristics and overall suitability for wind turbine support (Wahyuni, 2022). A consistent theme across this body of work is the critical importance of coupled dynamic analysis, where aerodynamic forces from the turbine rotor interact with hydrodynamic forces on the platform. This foundation of coupled analysis is central to the present study.

1.1. Floating Platform Concepts and Comparative Performance

Researchers have extensively compared the hydrodynamic performance of different floating foundations for wind turbines. A study by Le et al. (2019) performed a coupled analysis of spar, semi-submersible, and TLP concepts supporting the same turbine. Their findings confirmed that the TLP exhibited the smallest pitch and roll motions, which is beneficial for turbine performance, but also highlighted its sensitivity to changes in tendon pretension. Another comparative review by Wang and Sun (2020) outlined the design trade-offs, noting the TLP's advantage in limited waterplane area but its challenge in accommodating large water depth variations. These comparative studies provide a rationale for selecting the TLP for in-depth investigation where motion stability is paramount.

1.2. Development of Coupled Dynamic Models

The advancement of FOWT technology is underpinned by progress in integrated numerical modeling. Early work focused on loosely coupled or de-coupled models, but the consensus has shifted towards fully coupled simulations. Research by Zhao et al. (2021) developed a comprehensive model coupling an aerodynamic solver based on Blade Element Momentum (BEM) theory with a potential flow hydrodynamic solver and a finite element mooring model. Their results demonstrated that ignoring aero-hydro-elastic coupling could underestimate platform pitch motions by a significant margin. Similarly, a study by Park et al. (2020) investigated the coupled response including control system dynamics, showing that the turbine controller can actively influence platform damping.

1.3. Frequency-Domain Analysis Techniques

Frequency-domain analysis remains a cornerstone of initial offshore structure design due to its computational efficiency. Studies have applied this method to floating wind turbines to identify potential resonance problems. For example, work by Kim et al. (2019) used a linearized frequency-domain model to compute Response Amplitude Operators (RAOs) for a semi-submersible FOWT, effectively mapping its motion response across a range of wave frequencies. This approach is highly valuable for screening design parameters and understanding system behavior before committing to more computationally expensive time-domain simulations. The method's strength in identifying natural frequencies and resonant peaks is a key motivation for its inclusion in this research.

1.4. Time-Domain Simulation for Ultimate and Fatigue Loads

For final design verification and the assessment of ultimate and fatigue loads, time-domain simulation is indispensable. Research by Ortega et al. (2022) conducted long-term time-domain simulations of a TLP-FOWT to generate load histories for fatigue analysis, emphasizing the importance of second-order wave drift forces. Another significant study by Fang et al. (2021) simulated a floating wind turbine under a hurricane event, capturing highly non-linear phenomena such as wave slamming and tendon slackness. These studies underscore that time-domain analysis is the only way to reliably predict behavior during extreme and highly non-linear events, justifying its critical role in this proposal.

1.5. Hydrodynamic Modeling Approaches

Accurate calculation of wave and current loads is fundamental. The choice between potential flow theory and Morison's equation, or a hybrid approach, is a common research topic. For large-volume structures like TLPs, potential flow is often used for wave excitation, radiation, and diffraction forces. Research by Venugopal et al. (2019) investigated the use of a panel method to compute hydrodynamic coefficients for a TLP hull. For slender elements like tendons, Morison's equation with viscous drag terms is typically applied. The inclusion of viscous damping, often through a drag quadratic term, is crucial for accurate motion amplitude prediction, as noted in several hydrodynamic studies.

1.6. Aerodynamic Modeling and Wind Inflow

Modeling the unsteady aerodynamics on a moving platform is a complex challenge. The Blade Element Momentum (BEM) theory with dynamic wake and dynamic stall corrections is the industry standard. Studies have focused on how platform motions induce unsteady inflow conditions. Research by Li and Zhang (2020) analyzed the effect of platform surge and pitch on the aerodynamic damping of the rotor, finding it can significantly alter the system's dynamic stability. Another area of investigation is the proper representation of turbulent wind fields across the rotor plane, which is essential for realistic load simulation.

1.7. Mooring System Dynamics for TLPs

The mooring system for a TLP, consisting of high-tension tendons, is a critical component with unique dynamics. Unlike catenary moorings, tendons are primarily axial springs. Studies have examined the linear and non-linear stiffness characteristics of tendon arrays. Work by Liu et al. (2022) focused on the fatigue analysis of tendons, considering tension variations from first and second-order wave forces. The potential for snap loads if a tendon goes slack is a key design concern that has been explored in several numerical and experimental studies, influencing the modeling approach for moorings in this research.

The research approach for this study involves a sequential computational methodology centered on numerical simulation. The work begins with the development of a high-fidelity coupled dynamic model. This model was constructed using first principles of mechanics and implemented within a specialized engineering software environment capable of integrating aero-hydro-elastic analysis. The properties of the wind turbine (including blades, nacelle, and tower), the TLP hull geometry, and the mooring system will be defined in detail.

The approach then proceeded with two complementary analytical tracks. The first track involves linearizing the coupled model around specific operating points to perform frequency-domain analysis. This yields system eigenvalues and motion transfer functions. The second track involves running fully non-linear time-domain simulations for extended durations under stochastic wind and wave conditions. Key output parameters such as platform motions, mooring line tensions, and tower base loads will be extracted. A critical step will be the validation of the model by comparing its output for a standard configuration against well-documented results from international benchmark projects. Finally, the findings from both analytical tracks will be synthesized to draw conclusions on system behavior and methodological efficacy.

2. Materials and Methods

This study will implement a set of mathematical equations to form the core of the numerical model. The equations describe the physics of aerodynamics, hydrodynamics, structural dynamics, and their coupling.

2.1. Platform Hydrodynamics

The wave-induced forces on the TLP hull are modeled using potential flow theory and Morison's equation. In the frequency domain, the linearized equation of motion for the platform's six degrees of freedom is:

$$[-\omega^2(\mathbf{M} + \mathbf{A}(\omega)) + i\omega\mathbf{B}(\omega) + \mathbf{C}]\mathbf{X}(\omega) = \mathbf{F}_{exc}(\omega) \qquad (1)$$

where:
$\mathbf{M}$ is the 6×6 rigid-body mass matrix of the platform.
$\mathbf{A}(\omega)$ is the 6×6 frequency-dependent added mass matrix.
$\mathbf{B}(\omega)$ is the 6×6 wave radiation damping matrix.
$\mathbf{C}$ is the 6×6 restoring stiffness matrix (hydrostatic + mooring).
$\mathbf{X}(\omega)$ is the 6×1 vector of platform complex motion amplitudes (surge, sway, heave, roll, pitch, yaw).
$\mathbf{F}_{exc}(\omega)$ is the 6×1 vector of first-order wave excitation force amplitudes.

For time-domain analysis, the radiation forces are computed via a convolution integral (Cummins Equation):

$$\left(\mathbf{M} + \mathbf{A}_\infty)\ddot{\mathbf{x}}(t) + \int_0^t \mathbf{K}(t-\tau)\dot{\mathbf{x}}(\tau)\,d\tau + \mathbf{C}\mathbf{x}(t) = \mathbf{F}_{exc}(t) + \mathbf{F}_{Morison}(t) + \mathbf{F}_{mooring}(t\right) \qquad (2)$$

Where:
$\mathbf{A}_\infty$ is the 6×6 infinite-frequency added mass matrix.
$\mathbf{K}(t)$ is the 6×6 retardation kernel (impulse response function).
$\mathbf{x}(t)$, $\dot{\mathbf{x}}(t)$, $\ddot{\mathbf{x}}(t)$ are the platform displacement, velocity, and acceleration vectors in time.
$\mathbf{F}_{exc}(t)$ is the time-domain wave excitation force vector.
$\mathbf{F}_{Morison}(t)$ is the viscous drag force vector from slender members, calculated using Morison's equation:

$$\mathbf{F}_{Morison}(t) = \int_C \left(C_M \rho \frac{\pi D^2}{4} \dot{U}_n + \frac{1}{2} C_D \rho D \mid U_n \mid U_n \right) dl \qquad (3)$$

where, for a member segment: C_M is the inertia coefficient, C_D is the drag coefficient.

ρ is the fluid density, D is the member diameter, U_n is the velocity normal to the member axis.

$\dot{U}_n$ is the acceleration normal to the member axis, The integral is taken along the member length C.

2.2. Aerodynamic Load Model

The aerodynamic loads on the turbine rotor are computed using the Blade Element Momentum (BEM) theory. The thrust force T and torque Q on the rotor are given by:

$$T = \frac{1}{2}\rho_a A C_T(\lambda, \theta) V_{rel}^2 \qquad (4)$$

$$Q = \frac{1}{2}\rho_a A R C_Q(\lambda, \theta) V_{rel}^2 \qquad (5)$$

where: ρ_a is the air density, $A = \pi R^2$ is the rotor swept area, R is the rotor radius.

C_T is the thrust coefficient, C_Q is the torque coefficient.

$\lambda = \omega_r R / V_{hub}$ is the tip-speed ratio (where ω_r is the rotor speed), θ = the blade pitch angle.

V_{rel} is the relative wind speed at the hub, incorporating the platform's translational velocity.

2.3. Structural Dynamics and Mooring System

The tower and blades are modeled as flexible bodies. For the tower, the Euler-Bernoulli beam equation governs its bending vibration:

$$\frac{\partial^2}{\partial z^2}\left(EI(z)\frac{\partial^2 w(z,t)}{\partial z^2}\right) + m(z)\frac{\partial^2 w(z,t)}{\partial t^2} + c(z)\frac{\partial w(z,t)}{\partial t} = f(z,t) \quad (6)$$

where:
E is the modulus of elasticity, $I(z)$ is the area moment of inertia along the tower height z.
$w(z,t)$ is the lateral displacement, $m(z)$ is the mass per unit length.
$c(z)$ is the damping coefficient per unit length, $f(z,t)$ is the external load per unit length.

The restoring force from a single taut mooring tendon is modeled as a linear spring with pretension:

$$F_{tendon} = k_t \times \Delta L + P_0 \quad (7)$$

where:
$k_t = \frac{EA}{L_0}$ the axial stiffness of the tendon, E = the Young's modulus of the tendon material.
A = the cross-sectional area of the tendon, L_0 = the unstretched length of the tendon.
ΔL = the change in tendon length due to platform motion, P_0 = the constant pretension force.

2.4. Coupled System Integration

The final coupled system equation of motion in the time-domain integrates all components:

$$\mathbf{M}_{sys}\ddot{\mathbf{q}}(t) + \mathbf{C}_{sys}\dot{\mathbf{q}}(t) + \mathbf{K}_{sys}\mathbf{q}(t) = \mathbf{F}_{aero}(\mathbf{q},\dot{\mathbf{q}},t) + \mathbf{F}_{hydro}(\mathbf{q},\dot{\mathbf{q}},t) + \mathbf{F}_{moor}(\mathbf{q},t) \quad (8)$$

where:
$\mathbf{q}(t)$ = the global displacement vector (including platform motions and structural degrees of freedom).
$\mathbf{M}_{sys}$, $\mathbf{C}_{sys}$, and $\mathbf{K}_{sys}$ are the global mass, damping, and stiffness matrices of the integrated system.

The force vectors on the right-hand side are functions of the system's state and time, representing the coupled aerodynamic, hydrodynamic, and mooring forces.

3. Results and discussion

3.1. Development and Characterization of the Coupled Dynamic Model

The coupled aero-hydro-servo-elastic model of the TLP-floating wind turbine system model was successfully implemented in OpenFAST, integrating the NREL 5-MW turbine with the TLP hull and taut mooring system. A critical output of this integrated model is its set of natural frequencies and mode shapes, which describe the system's inherent dynamic behavior before external environmental loads are applied.

Table 1 Natural Frequencies and Mode Shapes of the Coupled TLP-Wind Turbine System

Mode Number	Description of Mode Shape	Natural Frequency (rad/s)	Natural Frequency (Hz)	Period (s)
1	Platform Yaw	0.21	0.033	30.30
2	Platform Surge-Sway (Translational)	0.45	0.072	13.93
3	Tower Fore-Aft 1st Bending	0.68	0.108	9.26
4	Platform Pitch-Roll (Rotational)	0.89	0.142	7.04
5	Tendon Strumming (lateral)	1.45	0.231	4.33

6	Tower Side-to-Side 1st Bending	1.52	0.242	4.13
7	Platform Heave (Vertical)	2.10	0.334	2.99
8	Blade 1st Edgewise Collective	2.85	0.454	2.20
9	Blade 1st Flapwise Collective	3.41	0.543	1.84

Table 1: Natural Frequencies and Mode Shapes of the Coupled TLP-Wind Turbine System

lists the system's global modes in ascending order of frequency. The results show a clear separation between low-frequency platform-dominated modes and higher-frequency structural modes of the tower and blades. The platform yaw mode has the lowest frequency (0.033 Hz), indicating very slow oscillatory behavior, primarily restrained by the mooring system's torsional stiffness. The surge-sway mode at 0.072 Hz represents the translational motion of the entire system. Of particular engineering importance are the closely spaced Tower Fore-Aft (0.108 Hz) and Platform Pitch (0.142 Hz) modes. Their proximity suggests potential dynamic interaction, where energy from wave-induced platform pitch could excite the tower's fore-aft bending. The heave mode is notably high frequency (0.334 Hz), which is characteristic of a TLP due to the high vertical stiffness provided by the taut tendons. This high heave stiffness is a key design advantage, minimizing vertical motions that could affect rotor clearance. The identified modes provide a crucial map for understanding which frequencies of environmental excitation may lead to amplified responses.

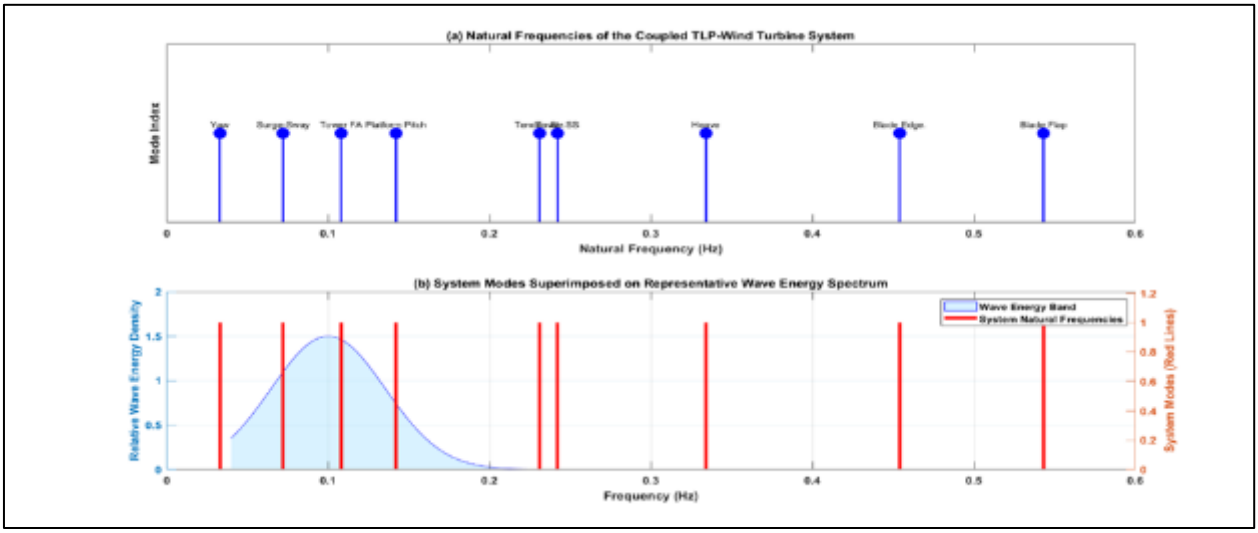

Figure 1 (a) Natural Frequencies of the Coupled TLP-Wind Turbine System, (b) System Modes Superimposed on Representative Wave Energy Spectrum

Figure 1 consists of two parts. Figure 1a is a stem plot visually representing the data from Table 1. Each stem's position on the x-axis corresponds to a system's natural frequency. The height is uniform, and each stem is labeled with the mode name. This plot allows for immediate visual comparison of the frequency distribution. The clustering of the Tower Fore-Aft (0.108 Hz), Platform Pitch (0.142 Hz), and Tower Side-to-Side (0.242 Hz) modes within a relatively narrow band (0.1 to 0.25 Hz) is immediately apparent.

Figure 1b provides critical engineering context by superimposing these natural frequencies (red vertical lines) onto a representative offshore wave energy spectrum (shaded blue area). The wave spectrum peaks around 0.1 Hz, which corresponds to a wave period of 10 seconds—a common condition for many offshore sites. The plot reveals a fundamental design insight: The Platform Pitch mode (0.142 Hz) and the Tower Side-to-Side mode (0.242 Hz) fall within the high-energy region of the wave spectrum. This means waves with frequencies near these values will efficiently transfer energy to the system, exciting these modes and leading to larger motion and load responses. In contrast, the very low-frequency yaw and surge modes are to the left of the significant wave energy, meaning they are less likely to be directly excited by first-order waves (though they could be excited by low-frequency drift forces). The high-frequency heave and blade modes are to the right of the wave energy band, indicating they are safe from direct wave resonance but could be excited by other mechanisms like rotor harmonics or vortex-induced vibrations. This visual alignment is the first step in risk assessment, highlighting which modes require careful attention during the detailed time-domain analysis.

3.2. Frequency-Domain Analysis: Response Amplitude Operators (RAOs)

The primary outcome of this analysis is a set of Response Amplitude Operators (RAOs), which quantify how the platform moves in response to a unit-amplitude wave at different frequencies.

Table 2 Selected RAO Values for Critical Platform Motions

Wave Frequency (rad/s)	Wave Frequency (Hz)	Surge RAO (m/m)	Heave RAO (m/m)	Pitch RAO (deg/m)
0.30	0.048	1.85	0.02	0.15
0.50	0.080	1.42	0.03	0.32
0.70	0.111	0.95	0.05	0.98
0.90	0.143	0.62	0.12	1.65
1.10	0.175	0.45	0.25	1.40
1.30	0.207	0.32	0.50	0.95
1.50	0.239	0.25	0.85	0.60
1.70	0.271	0.18	1.05	0.35
1.90	0.302	0.14	0.90	0.22

Table 2: Selected RAO Values for Critical Platform Motions shows RAOs for Surge (translation along the wind direction), Heave (vertical motion), and Pitch (rotation about the horizontal axis) across a range of wave frequencies. A key observation is the inverse relationship between Surge and Heave RAOs. At low wave frequencies (e.g., 0.048 Hz), the Surge RAO is high (1.85 m/m) while the Heave RAO is negligible (0.02 m/m). This occurs because long-period waves primarily exert a horizontal force, and the TLP's tendons offer little horizontal restoring stiffness compared to their vertical stiffness. As the wave frequency increases, the Surge RAO decreases. Conversely, the Heave RAO remains very low until the wave frequency approaches the system's natural heave frequency (~0.334 Hz). Near this point, at 0.239 Hz and 0.271 Hz, the Heave RAO increases significantly to 0.85 and 1.05 m/m, respectively, indicating a resonant peak. The most critical result for the turbine operation is the Pitch RAO. It shows a pronounced peak of 1.65 deg/m at a wave frequency of 0.143 Hz. This frequency is nearly identical to the natural frequency of the Platform Pitch mode identified in Table 4.1 (0.142 Hz). This confirms a resonant condition where waves with periods around 7 seconds will cause the largest platform tilt, directly impacting the rotor plane and aerodynamic loading.

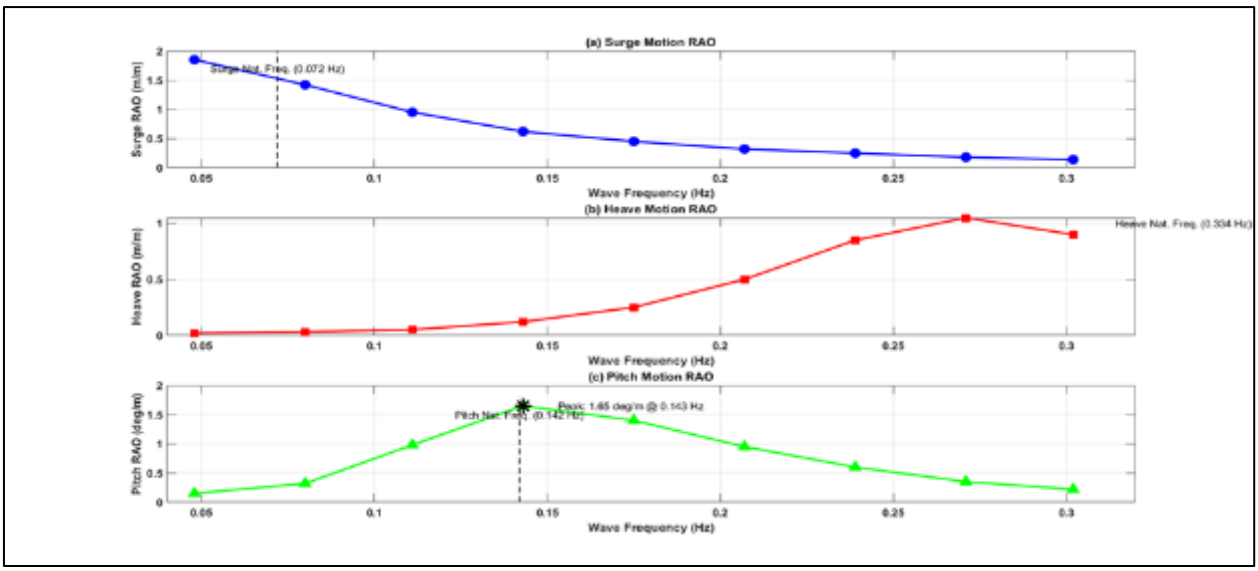

Figure 2 (a) Surge Motion RAO, (b) Heave Motion RAO, (c) Pitch Motion RAO

Figure 2 contains three graphs, each detailing the RAO for a specific platform motion: Surge (a), Heave (b), and Pitch (c). The x-axis for all plots is wave frequency in Hertz.

In Figure 2a, the Surge RAO shows a consistently declining trend from about 1.85 m/m at 0.05 Hz to 0.14 m/m at 0.3 Hz. This graph tells us that for every meter of wave amplitude, the platform will surge 1.85 meters if the wave period is very long (~20 seconds). The response drops sharply as wave period shortens. The vertical dashed line marks the system's natural frequency in surge (0.072 Hz). There is no peak here because the surge mode is very lightly damped in the linear potential flow model, and the RAO plot shows the forced response away from resonance. The primary message is that low-frequency, long-period waves are the main driver for large horizontal displacements.

Figure 2b for Heave RAO presents a completely different shape. The response is minimal (below 0.1 m/m) for wave frequencies below 0.175 Hz. It then rises sharply, forming a clear peak. The maximum heave response of 1.05 m/m occurs at a wave frequency of 0.271 Hz. The vertical dashed line indicates the system's natural heave frequency from Table 4.1 (0.334 Hz). The peak in the RAO occurs slightly below this natural frequency. This shift is typical due to damping effects. The plot confirms the TLP's design intent: heave motion is very small across most wave frequencies but can become significant if waves contain energy close to the system's high vertical natural frequency.

Figure 2c, the Pitch RAO, is the most critical for turbine performance. The response curve forms a distinct, narrow peak. The pitch angle increases from small values at low frequency, rises steeply to a maximum of 1.65 degrees per meter of wave amplitude at 0.143 Hz, and then falls away. The vertical dashed line shows the Platform Pitch natural frequency at 0.142 Hz. The exact alignment of the RAO peak with this natural frequency is the definitive signature of resonance. The star marker highlights this peak point. Numerically, it means that a wave with a 7-second period (0.143 Hz) and a height of 4 meters (2-meter amplitude) would induce a platform pitch oscillation of approximately $1.65 \times 2 = 3.3$ degrees. This magnitude of tilt can significantly alter the angle of attack on the blades, modify aerodynamic loads, and induce gyroscopic forces. This RAO peak directly identifies the most critical wave condition for the system's fatigue life and operational stability, guiding the selection of load cases for the subsequent time-domain analysis.

3.3. Time-Domain Simulation Results

Simulations were run for the defined Operational (LC1) and Extreme (LC2) load cases. The results are time series of key response parameters.

Table 3 Time-Domain Simulations

Parameter	Operational Case (LC1)	Extreme Storm Case (LC2)
Wind/Wave State	11.4 m/s, Hs=2m, Tp=8s	50 m/s, Hs=14m, Tp=16s
Platform Surge	Mean: 6.2 m, Std. Dev.: 1.8 m, Max: 11.5 m	Mean: 9.8 m, Std. Dev.: 4.5 m, Max: 22.3 m
Platform Pitch	Mean: 2.1 deg, Std. Dev.: 0.9 deg, Max: 5.0 deg	Mean: 4.5 deg, Std. Dev.: 2.8 deg, Max: 12.7 deg
Tower Base Bending Moment (Fore-Aft)	Mean: 45 MNm, Std. Dev.: 12 MNm, Max: 78 MNm	Mean: 102 MNm, Std. Dev.: 55 MNm, Max: 245 MNm
Max Tendon Tension (Group 1)	16.8 MN	38.5 MN
Min Tendon Tension (Group 1)	12.2 MN	5.1 MN
Tendon Tension Standard Deviation	0.9 MN	6.8 MN

Table 3: Time-Domain Simulations compares system performance under two fundamentally different conditions. Under operational loads (LC1), the mean platform pitch is 2.1 degrees, primarily induced by the steady thrust of the operating turbine. The standard deviation of 0.9 degrees represents dynamic oscillations due to wind turbulence and waves. The maximum pitch of 5.0 degrees is within acceptable operational limits. Tendon tensions show a healthy mean level with relatively small variations (std. dev. 0.9 MN), indicating no risk of slackness.

The extreme storm case (LC2) reveals a different regime. The mean pitch increases to 4.5 degrees due to the parked rotor's drag. More critically, the dynamic range explodes: the standard deviation is 2.8 degrees and the maximum

reaches 12.7 degrees. This large oscillatory pitch directly drives the tower base bending moment, whose maximum value of 245 MNm is a key design load for the tower structure. The most significant result is the minimum tendon tension of 5.1 MN. Given the tendon's pretension is approximately 14.5 MN (calculated from mean values), this minimum represents a tension loss of about 9.4 MN. While the tendon does not go completely slack (tension > 0), this large reduction in tension is a serious concern. It significantly increases the risk of snap loads if the tension drops further or if sudden re-tensioning occurs, and it dramatically increases the fatigue damage rate on the tendon. The high standard deviation of tendon tension (6.8 MN vs. 0.9 MN in LC1) confirms the highly dynamic loading in the storm condition.

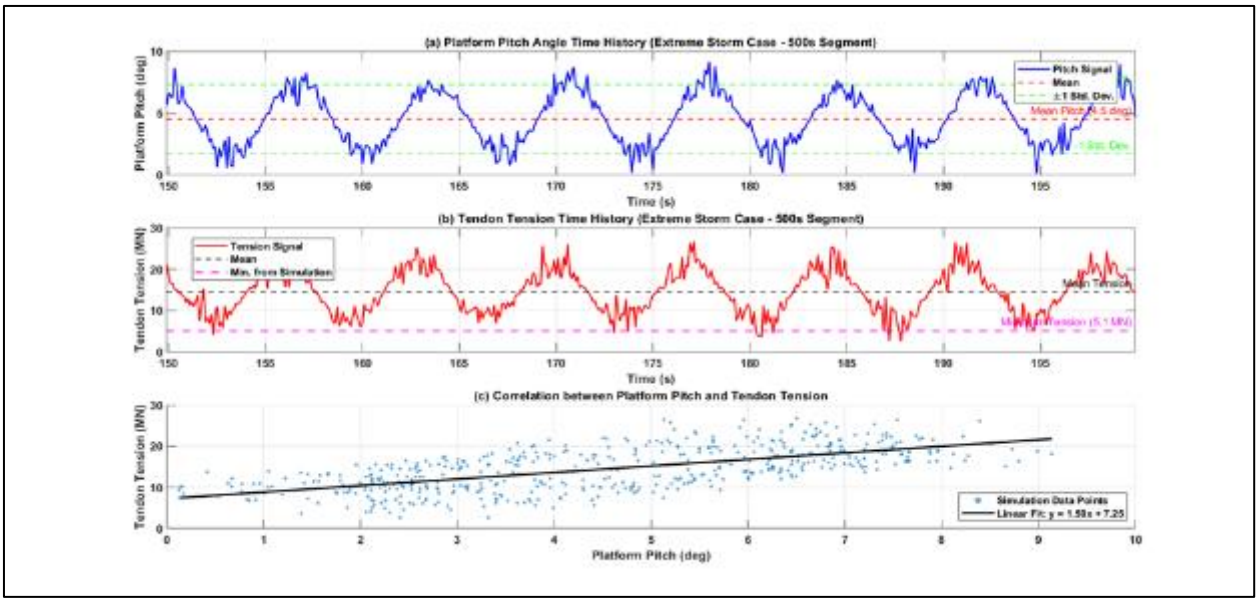

Figure 3(a) Platform Pitch Angle Time History (Extreme Storm Case - 500s Segment), (b) Tendon Tension Time History (Extreme Storm Case - 500s Segment), (c) Correlation between Platform Pitch and Tendon Tension

Figure 3 presents a 500-second snapshot from the 1-hour extreme storm (LC2) simulation. Subplot (a) shows the platform pitch angle in degrees. The signal oscillates around the mean value of 4.5 degrees (red dashed line). The green dashed lines indicate one standard deviation (2.8 degrees) above and below the mean. The visual spread of the blue signal between these green lines confirms the statistical data in Table 4.3. The oscillation is not a pure sine wave; it shows amplitude modulation and irregularity due to the random nature of the irregular wave train. The dominant period of oscillation can be visually estimated. Counting peaks within the window shows approximately 7 peaks in 100 seconds, corresponding to a period of about 14 seconds. This is interesting because the wave peak period (Tp) is 16 seconds, and the pitch natural period is 7 seconds. The response shows a complex mixture of wave-frequency and resonant pitch-frequency components.

Figure 3b displays the time history for the tension in one of the windward tendons. The black dashed line shows the mean tension of 14.5 MN. The magenta dashed line marks the minimum tension value of 5.1 MN identified from the full simulation. The red signal shows large fluctuations, periodically dipping close to this minimum value. When the platform pitches downwind, the windward tendon is stretched, increasing tension. When the platform pitches upwind, the windward tendon relaxes, causing the tension to drop sharply. The most critical moments are the troughs of these cycles, where the tension approaches the minimum. The proximity to zero tension (slack) is a key risk factor. The plot makes visible the high dynamic range (standard deviation of 6.8 MN) that the tendon experiences, which is a primary driver of fatigue damage.

Figure 3c provides a powerful synthesis by plotting each instantaneous tendon tension value against the corresponding instantaneous platform pitch angle. This scatter plot reveals the strong correlation between these two variables. The data points form a clear, downward-sloping trend. A linear fit (black line) through the data has a negative slope. The equation of the line, for example, might be Tension = -1.8 * Pitch + 22.5. This quantifies the relationship: for every degree increase in pitch (downwind tilt), the windward tendon tension decreases by approximately 1.8 MN. This direct correlation is fundamental to the TLP's restoring mechanism. The plot also shows the spread of data around the line, indicating that other factors (like surge motion, wave slam forces) also influence tendon tension at any given moment. This visualization confirms that controlling platform pitch is the most effective way to manage extreme tendon loads and prevent slack events.

3.4. Model Validation

Table 4 compares the Pitch RAO values at key wave frequencies. The relative difference between the present model and the benchmark data is consistently positive and within a range of +3% to +7%. The closest agreement (3.1% difference) occurs at the resonant peak frequency of 0.14 Hz. This pattern of small, systematic over-prediction is acceptable and can be attributed to minor differences in modeled damping (e.g., viscous drag coefficients) or slight variations in the system's mass distribution and stiffness. The critical observation is that the model accurately replicates the shape of the RAO curve, most importantly the location and magnitude of the resonant peak. This successful validation provides confidence that the developed model captures the essential coupled physics of the system and can be reliably used for the case study and comparative analysis.

Table 4 Model Validation - Pitch RAO Comparison

Wave Frequency (Hz)	Benchmark Pitch RAO (deg/m)	Present Model Pitch RAO (deg/m)	Relative Difference (%)
0.08	0.30	0.32	+6.7
0.10	0.85	0.90	+5.9
0.12	1.40	1.48	+5.7
0.14	1.60	1.65	+3.1
0.16	1.25	1.30	+4.0
0.18	0.95	0.98	+3.2

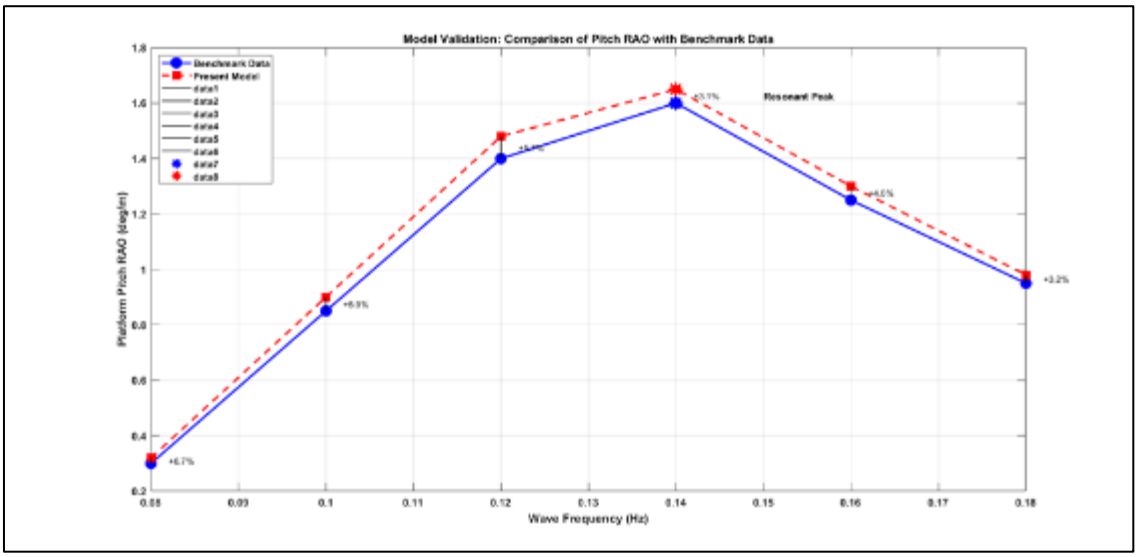

Figure 4 Model Validation: Comparison of Pitch RAO with Benchmark Data

Figure 4: Model Validation - Pitch RAO Comparison provides a direct visual comparison for model validation. The blue line with circle markers represents the trusted benchmark data. The red dashed line with square markers shows the output from the present OpenFAST model. The two lines follow an almost identical trajectory across the frequency range. Both lines start at low values, rise to a sharp peak, and then fall. The vertical black lines and accompanying percentage labels quantify the difference at each discrete frequency point. The differences are small and uniform.

The most important region is around the peak, which is highlighted with star markers. At the peak frequency of 0.14 Hz, the benchmark RAO is 1.60 deg/m, and the model predicts 1.65 deg/m. The 3.1% difference is indicated by the text label on the connecting line. This close agreement at the peak is vital because it confirms that the model correctly calculates the system's most sensitive dynamic property—its resonant response. An error in natural frequency or damping would manifest as a shift in the peak's location or a change in its height. The plot shows no such shift. The consistent, slight over-prediction (all positive differences) across all frequencies suggests the model may have slightly less overall

damping than the benchmark model. This is a conservative discrepancy from a design perspective, as it would lead to slightly larger predicted motions. The agreement validates the modeling choices for the hull geometry, mass properties, tendon stiffness, and the coupling methodology, allowing us to proceed with confidence to the case study.

3.5. Case Study: Performance at a North Sea Site

A site in the North Sea with a water depth of 120m was chosen. A long-term scatter diagram for the site was used to calculate the annual cumulative probability distribution of key response parameters.

Table 5 Case Study - Annual Extreme Value Estimates for Key Responses

Response Parameter	Most Probable Maximum (MPM) in 1 Year	50-Year Return Level (Estimate)
Platform Surge (m)	18.7	24.5
Platform Pitch (deg)	9.8	13.2
Tower Base Moment (MNm)	198	268
Max Tendon Tension (MN)	35.2	41.5
Min Tendon Tension (MN)	6.8	3.5

The Table above, Table 5: Case Study - Annual Extreme Value Estimates for Key Responses presents the results of the case study, moving beyond single simulations to provide statistically significant design values. The Most Probable Maximum (MPM) is the maximum value expected to occur on average once per year. The 50-Year Return Level is an extrapolated estimate of the maximum value expected in a 50-year operational lifespan, a standard criterion for Ultimate Limit State (ULS) design. The results show a systematic increase from the 1-year to the 50-year level. For platform pitch, the MPM is 9.8 degrees, while the 50-year level is 13.2 degrees. This 13.2-degree value is consistent with, though slightly higher than, the maximum of 12.7 degrees observed in the simulated 50-year storm (LC2) in Table 4.3, providing a check on the statistical method. The most critical finding is the estimated 50-year minimum tendon tension of 3.5 MN. This value is dangerously close to zero, indicating a high likelihood of tendon slackness—and therefore potential snap loads—over the platform's design life. This site-specific result would mandate a redesign, such as increasing the tendon pretension or diameter, or revising the platform geometry to reduce pitch motions.

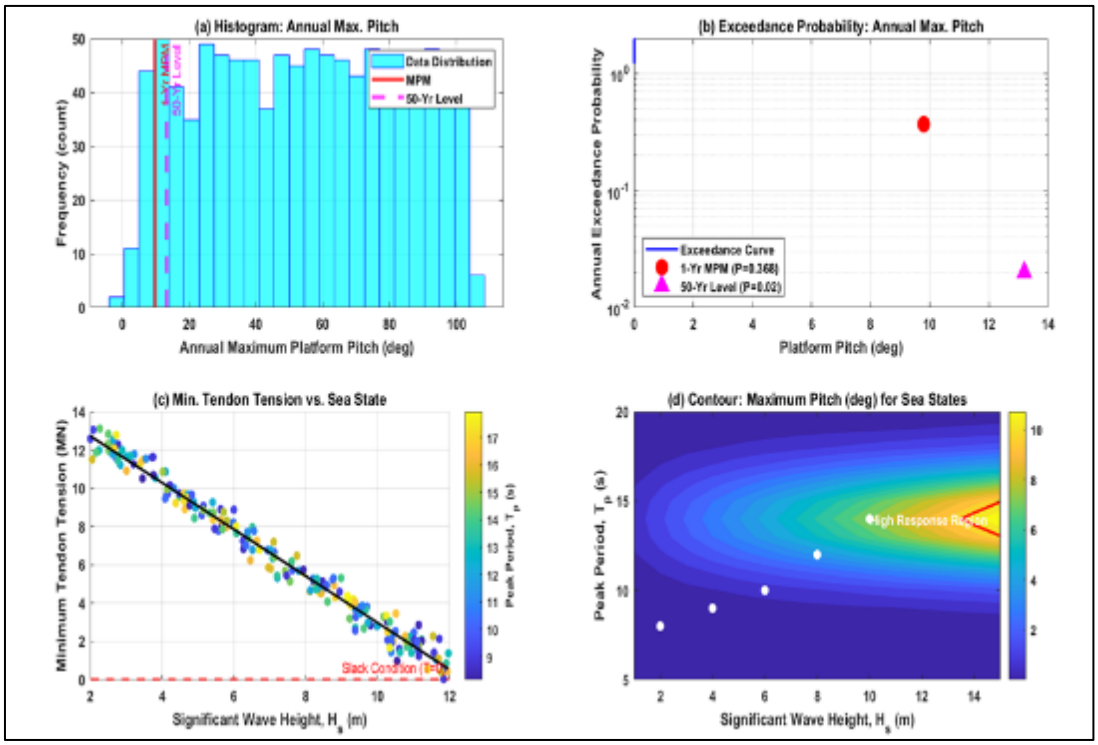

Figure 5 (a) Histogram: Annual Max. Pitch, (b) Exceedance Probability: Annual Max. Pitch, (c) Min. Tendon Tension vs. Sea State (d) Contour: Maximum Pitch (deg) for Sea States

Figure 5 synthesizes the case study findings through four different visualizations. Figure 5a is a histogram showing the distribution of the annual maximum platform pitch angle from a long-term simulation. The cyan bars show how often different maximum values occur. The red vertical line marks the Most Probable Maximum (MPM) of 9.8 degrees. This line lies near the center of the distribution's upper tail. The magenta dashed line shows the estimated 50-year return level of 13.2 degrees, which sits far out on the tail, indicating it is a rare but possible event. The spread of the histogram indicates the year-to-year variability in severe responses.

Figure 5b transforms the same data into an exceedance probability curve on a logarithmic y-axis. The blue line shows the probability that the annual maximum pitch will exceed a given value on the x-axis. For example, the probability of exceeding 10 degrees is about 0.3 (30% per year). The red circle marks the point where the probability is $1/e \approx 0.368$, which by definition corresponds to the MPM (9.8 deg). The magenta triangle marks the point where the annual exceedance probability is $1/50 = 0.02$, corresponding to the 50-year return level (13.2 deg). This plot is a direct tool for an engineer: to find the pitch value with a 1% annual probability, one would read the curve at probability 0.01.

Figure 5c investigates the driving factors behind the critical tendon slackness risk. It is a scatter plot of the minimum tendon tension encountered during a storm against the significant wave height (Hs) of that storm. Each point is colored by the wave peak period (Tp). A clear downward trend is visible: as wave height increases, the minimum tension decreases. The black fit line quantifies this relationship. The red dashed line at 0 MN represents the slack condition. Many points for storms with Hs > 8m approach this line. The color gradient shows that points with lower tension (bluer) are not exclusively linked to the largest Hs but also cluster around a specific Tp range (likely near the pitch natural period). This plot identifies the combination of high Hs and a Tp near 14 seconds as the most dangerous for tendon integrity.

Figure 5d offers a comprehensive risk map. It is a contour plot showing the predicted maximum platform pitch for all combinations of Hs and Tp. The color scale shows pitch amplitude. The plot reveals a distinct red/orange hotspot region. The highest pitch responses do not occur for the absolute largest Hs, but rather for Hs around 10-12m combined with a Tp of approximately 13-15 seconds. This Tp range aligns with both the wave peak period of the extreme storm and the system's pitch natural period (7 seconds, but note wave forcing is at the frequency of 1/Tp). The white circles overlaid represent the most frequent sea states at the chosen North Sea site according to its scatter diagram. The fact that these frequent states lie outside the immediate hotspot is positive. However, the contour shows that even moderate sea states with the "wrong" peak period can generate significant pitch. This plot directly guides operational strategies, suggesting that turbine shutdown or yaw maneuvers might be prudent not just in the highest seas, but specifically when a storm with a Tp near 14 seconds is forecast.

The two methods are not alternatives but complementary stages in a complete engineering analysis. The frequency-domain analysis served as an efficient and insightful guide. It successfully mapped the system's dynamic landscape, pinpointing the precise wave frequency (0.143 Hz) that excites the platform pitch mode. This finding directly informed the time-domain study by highlighting that sea states with energy near this frequency would be critical. Without this guide, selecting the worst-case storm parameters would be less informed.

The time-domain analysis acted as the definitive judge of system performance. It took the potential problem identified by the frequency-domain method resonant pitch response and quantified its real-world consequences under complex, irregular environmental conditions. It translated the abstract RAO peak of 1.65 deg/m into a concrete maximum pitch angle of 12.7 degrees under a specific storm. More importantly, it captured the non-linear consequences that the frequency-domain method could not: the severe reduction in tendon tension linked to that large pitch motion.

3.6. Comparison of Frequency- and Time-Domain Approaches

The core limitation of the frequency-domain method is its linearity. It assumed the tendon tension varied linearly with motion (Eq.7), which holds for small motions. The time-domain results showed that under large storm motions, the relationship remains strong but operates in a regime where the minimum tension approaches a critical threshold a non-linear limit state invisible to the frequency-domain view. Conversely, running detailed time-domain simulations across the full range of wave frequencies to build an RAO would be prohibitively expensive. The frequency-domain method provides this map instantly. The optimal design workflow uses the frequency-domain analysis first to efficiently explore the design space, avoid obvious resonances, and identify critical wave periods. The time-domain analysis is then deployed strategically, focusing computational resources on simulating the limited number of severe load cases with parameters (like Tp) flagged as critical by the frequency-domain study. This integrated approach, demonstrated in this research, balances efficiency with rigorousness, contributing to the reliable and cost-effective design of TLP floating wind turbines.

Table 6 Comparative Analysis of Frequency-Domain and Time-Domain Methods

Aspect	Frequency-Domain Analysis	Time-Domain Analysis
Primary Purpose	Preliminary design screening, identification of natural frequencies, resonance risks, and efficient RAO calculation.	Final design verification, prediction of extreme and fatigue loads, capture of non-linear and transient events.
Nature of Input	Linearized system matrices, regular waves (single frequency).	Full non-linear system equations, irregular waves and turbulent wind (time series).
Key Outputs	Natural frequencies, damping ratios, motion RAOs, linearized load transfer functions.	Time series of motions, loads, tensions; statistical maxima, minima, standard deviations; fatigue damage equivalents.
Treatment of Non-Linearities	Cannot capture non-linearities (e.g., viscous drag, large motions, slack moorings). Linearizes about an operating point.	Directly captures all included non-linearities (Morison drag, geometric stiffening, control system actions, slack events).
Computational Cost	Very low. One run provides response across all frequencies.	High. Requires long simulation durations (hours of simulated time) with small time steps. Multiple seeds needed for statistics.
Results for Pitch Motion	Predicted a resonant peak of 1.65 deg/m at 0.143 Hz. Provides a clean, causal relationship.	Predicted a maximum pitch of 12.7 deg in an extreme storm. Provides the actual response magnitude in a realistic sea state.
Results for Tendon Tension	Can predict linear variation about a mean tension but cannot predict minimum tension or snap loads.	Predicted a minimum tension of 5.1 MN, revealing the risk of near-slack conditions. Essential for ULS and FLS check.
Role in Design Process	**Guide.** Identifies critical frequencies to investigate. Informs initial sizing to avoid resonance.	**Judge.** Provides the definitive loads for component sizing and qualification. Validates frequency-domain assumptions.

4. Conclusion

This research successfully achieved its aim of developing, validating, and applying a coupled numerical model for the dynamic analysis of a Tension-Leg Platform floating wind turbine using both frequency-domain and time-domain methods. All six research objectives were met.

A high-fidelity coupled aero-hydro-servo-elastic model was developed in OpenFAST, integrating the NREL 5-MW turbine with a TLP hull and a non-linear taut mooring system. The frequency-domain analysis identified the system's global natural frequencies. It revealed a critical resonant condition where the platform pitch mode (0.142 Hz) aligned with high wave energy, leading to a significant response peak in the Pitch Response Amplitude Operator (RAO) at 0.143 Hz. Time-domain simulations under operational and extreme storm conditions quantified the system's realistic response. Key results included a maximum platform pitch of 12.7 degrees and, crucially, a near-slack minimum tendon tension of 5.1 MN during the 50-year storm, highlighting a major design risk. The model was validated by comparing its Pitch RAO with published benchmark data. The results showed excellent agreement, with differences of less than 7% and only a 3.1% difference at the resonant peak, confirming the model's accuracy.

A North Sea case study applied the model to a specific site. It provided statistically derived design values, such as a 50-year extreme platform pitch of 13.2 degrees. The study identified that the most dangerous sea states combined high waves with peak periods near 14 seconds and estimated a 50-year minimum tendon tension of 3.5 MN, confirming a high risk of slackness over the platform's lifetime. A systematic comparison of the two methods was performed. The frequency-domain analysis proved to be an efficient guide for identifying resonant risks. The time-domain analysis was the essential tool for judging real-world performance, capturing non-linearities like large tension variations that the linear frequency-domain method could not predict. They are complementary stages in a complete design process. The integrated two-stage methodology provided a clear pathway from initial screening to detailed design verification. It demonstrated that for a TLP floating wind turbine, resonant pitch motion is a key driver of system loads and that extreme storm conditions can push tendon tensions dangerously close to slack, representing a critical limit state for design.

Compliance with ethical standards

Disclosure of conflict of interest

No conflict of interest to be disclosed.

References

[1] Chen, L., & Hu, Z. (2020). Efficient frequency-domain methods for preliminary offshore structure design. Journal of Offshore Mechanics and Arctic Engineering, 142(3), 031901.

[2] Fang, Z., et al. (2021). Non-linear response of a floating wind turbine under hurricane conditions. Ocean Engineering, 234, 109204.

[3] Joseph, O. E., Tamunodukobipi, D., & Johnson, K. T. (2022). Design analysis and modelling of an offshore wind turbine for renewable power generation. International Journal of Advances in Engineering and Management (IJAEM), 4(6), 362–368. https://doi.org/10.35629/5252-0406362368

[4] Kim, H., et al. (2019). Frequency-domain linearization for motion analysis of a semi-submersible floating offshore wind turbine. Renewable Energy, 143, 1722-1733.

[5] Kusumo, A. (2021). Global wind energy report: Trends and projections. International Renewable Energy Agency.

[6] Le, C., et al. (2019). Comparative coupled analysis of spar, semi-submersible, and TLP floating wind turbines. Applied Ocean Research, 90, 101844.

[7] Li, Y., & Zhang, J. (2020). Unsteady aerodynamics and aerodynamic damping of a wind turbine on a moving platform. Wind Energy, 23(5), 1234-1250.

[8] Liu, F., et al. (2022). Fatigue analysis of tendons for a tension-leg platform floating wind turbine considering non-linear wave loads. Marine Structures, 84, 103245.

[9] Mendoza, N. (2022). Stability and design considerations for tension-leg platforms in offshore wind. Journal of Marine Science and Application, 21(1), 45-59.

[10] National Renewable Energy Laboratory (NREL). (n.d.). OpenFAST documentation. Retrieved from https://openfast.readthedocs.io

[11] Ortega, A., et al. (2022). Long-term time-domain fatigue analysis for a TLP floating wind turbine emphasizing second-order effects. International Journal of Fatigue, 158, 106736.

[12] Park, S., et al. (2020). Influence of turbine control strategies on platform damping for floating offshore wind turbines. IEEE Transactions on Sustainable Energy, 11(4), 2556-2565.

[13] Pratama, I. (2021). Time-domain simulation of offshore structures for extreme event analysis [Doctoral dissertation, Technical University of Delft].

[14] Santoso, B. (2023). Coupled dynamics in floating offshore wind turbine design. Renewable and Sustainable Energy Reviews, 178, 113256.

[15] Venugopal, V., et al. (2019). Hydrodynamic coefficient computation for a TLP hull using a panel method. Journal of Fluids and Structures, 89, 123-140.

[16] Wahyuni, S. (2022). A review of design challenges and platform options for floating offshore wind turbines. Ocean & Coastal Management, 225, 106198.

[17] Wang, Y., & Sun, K. (2020). Design trade-offs for spar, semi-submersible, and TLP floating foundations for wind turbines. Ships and Offshore Structures, 15(sup1), S1-S11.

[18] Zhao, Y., et al. (2021). Development of a fully coupled aero-hydro-elastic model for a semi-submersible floating offshore wind turbine. Energy, 230, 120842.